POSSIBLE TIMING OF WRINKLE RIDGE FORMATION IN MARE TRANQUILLITATIS. T. Früh[1], H. Hiesinger[1], C. H. van der Bogert[1], N. Schmedemann[1] and L. Pauw[1], [1]Institut für Planetologie, Westfälische Wilhelms-Universität Münster, Wilhelm-Klemm-Str.10, 48149 Münster, Germany, (thomas.frueh@uni-muenster.de).

Introduction: Lunar wrinkle ridges exclusively occur within mare basins [1–3]. Their profile is typically asymmetric and consists of a broad arch and a superimposed irregular ridge [4,5]. However, they have a highly variable morphology and they regularly braid and rejoin along strikes [5]. Smaller secondary or even tertiary ridges commonly cap and flank larger primary ridges [6,7]. The wrinkle ridge surface texture often resembles an "elephant-hide" texture [8].

The timing of lunar wrinkle ridge formation is still being discussed and has implications for prevailing stress fields. Wrinkle ridges deform a broad range of maria units indicating a formation as early as ~3.8 Ga [9] and as recently as ~1.2 Ga [7]. [10] derived mean ages older than 3.0 Ga in a global survey of possible formation times for large wrinkle ridges. The high spatial resolution of the Narrow Angle Camera (NAC) on board the Lunar Reconnaissance Orbiter (LRO) enables further studies of different tectonic landforms, i.e., lobate scarps and wrinkle ridges. The abundance of boulder fields [11–13], the distinct crisp morphology, crosscutting relationships [14], crater counts [15], and associated small meter-scaled graben [16–18] allowed recent studies to propose tectonic activity within the last 100 Ma.

We mapped wrinkle ridges in Mare Tranquillitatis and studied their morphology on NAC images. In this study, we aim to get insights into the timing of lunar wrinkle ridge formation and their prevailing stress fields.

Methods: ArcGIS version 10.5.1. and QuickMap were used for mapping and analysis. Wrinkle ridges were mapped on Kaguya Terrain Camera (TC) images (pixel scale of ~ 10 m/pixel) at a scale of 1:80,000. Topographic information was gathered from the LRO LOLA – SELENE Kaguya DEM merge [19]. The highly variable morphology of wrinkle ridges demands the use of visual images, topographical data, hillshade maps, and slope maps for identifying wrinkle ridge structures. Polylines were drawn on top of continuous wrinkle ridge crest segments, independently of their order. We then used NAC images with incidence angles between 55° and 90° to study the wrinkle ridge morphologies. Wrinkle ridges were classified according to their morphology, general structure, surface texture, crosscut relationships, and the occurrence of small graben.

Results and Discussion: The mapping resulted in 802 wrinkle ridge segments, with a total length of ~8,364 km. Segments have a mean length of 10.4 km and range from 1.3 km to 81.8 km. On the basis of their morphology, the segments were classified into crisp, degraded, advanced degraded, and heavily degraded (Fig. 1) [similar to 18]. However, the transitions between these classes are gradual and transitional wrinkle ridges exist.

Crisp wrinkle ridges are typically small structures in terms of length and width. They have sharp edges and a distinctive and lobate morphology (Fig. 1). Craters with diameters of less than 50 m can be crosscut and only a few small craters are superimposed. Small (width < 50 m) crisp graben occur on top of and near these wrinkle ridges. Occasionally, boulders appear as patches.

Degraded wrinkle ridges are similar in size to the crisp wrinkle ridges. They have a winding and lobate morphology and their rounded edges are more indistinct than those of crisp wrinkle ridges (Fig. 1). While individual crosscut craters have diameters of less than 50 m, most crosscut craters show diameters of 100 m and more. Similar to crisp wrinkle ridges, superimposed craters are small and fewer in number relatively to the surrounding basalts and advanced and heavily degraded wrinkle ridges. Small graben rarely occur and display mostly rounded and degraded appearances. Boulder patches also appear occasionally, and extents vary from segment to segment.

The distinctive morphology of both crisp and degraded wrinkle ridges implies younger formation ages relatively to degraded and heavily degraded wrinkle ridges. The crosscutting of craters with diameters of less than 50 - 100 m suggests Copernican ages (< 800 Ma), based on survival times of lunar craters [20]. Small graben near lobate scarps and wrinkle ridges were interpreted as evidence for recent tectonic activity, since they are thought to result from uplift and flexural bending associated to movement of the underlying thrust fault [16–18]. Their widths can be below 10 m. Assuming infill rates of shallow depressions in lunar regolith of 5 ± 3 cm/Ma [21], a possible tectonic activity of crisp and some degraded wrinkle ridges during the last 50 Ma is suggested. Since not all degraded wrinkle ridges exhibit graben, they presumably formed between < 50 Ma to ~800 Ma.

Advanced and heavily degraded wrinkle ridges make up ~83% of all segments. They share similar distributions, morphologies, and are generally larger than crisp and degraded wrinkle ridges (Fig. 1). The

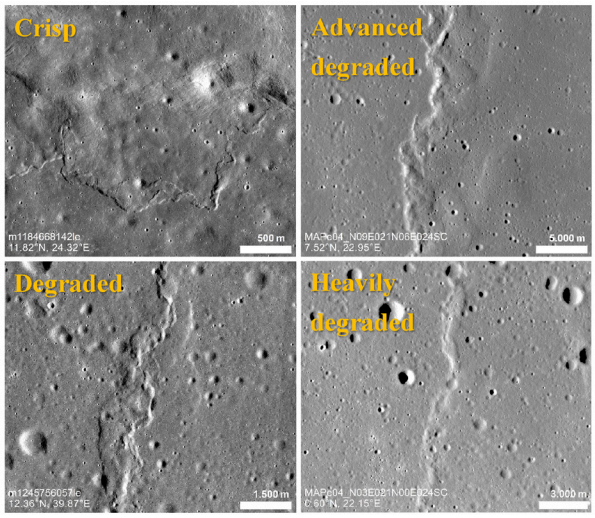

Figure 1. *NAC and TC images of wrinkle ridge segments from each degradation class.*

number and sizes of superimposed craters exceed those of the previously described classes, but their abundance is lower than for the surrounding mare units. If craters are crosscut, they have diameters of several hundred meters and more. Extensive boulder fields are distributed at the crests of some advanced degraded wrinkle ridges. The morphology of heavily degraded wrinkle ridges is diffuse (Fig. 1), and the crest and the broad arch are often only distinguishable in topographical data. Superimposed craters are very frequent and if crosscut craters are present, they have diameters of several hundred meters and more.

The deformation of all mare units defined by [22] suggests an upper age limit of at least 3.8 Ga for advanced and heavily degraded wrinkle ridges. The crosscutting of craters with diameters of several 100 m indicate Eratosthenian and/or Imbrian formation ages [20], resulting in formation ages ranging from ~3.8 Ga to ~800 Ma for both classes. However, boulder fields [11–13], crater counts [23,24] and the rare occurrence of small graben within the elephant-hide texture could hint to a possible activity within the last 100 Ma.

Conclusion and further Work: Wrinkle ridges in Mare Tranquillitatis show a broad range of possible formation ages ranging from ~3.8 Ga to < 50 Ma. Additional crater size frequency distribution (CSFD) and buffered crater counting (BCC) measurements are necessary for deriving individual wrinkle ridge model ages (AMA). A previous study suggested younger AMAs for wrinkle ridges in Mare Tranquillitatis compared to wrinkle ridges in other maria [10]. Therefore, further investigations of wrinkle ridge formation ages in different maria are necessary for a full understanding of the timing of wrinkle ridge formation.

The wrinkle ridge distribution in Mare Tranquillitatis differs from traditional patterns related to mascon tectonics [25] and reveals a presumably complex tectonic history, for which further studies are needed to uncover. Evidence for recent tectonic activity was previously found at lobate scarps in the lunar highlands [15,16] and also at wrinkle ridges in the lunar maria [12,14,18]. These signs are also present in Mare Tranquillitatis, highlighting recent widespread and global tectonic activity of the Moon. Global cooling, influenced by tidal forces, seems to be a likely candidate for creating a stress field, which is sufficient enough for shallow recent tectonic activity [26,27]. However, influences by regional stresses and combinations of different stress fields are possible. Hence, further studies are needed. The trigger behind the possible reactivity of ancient wrinkle ridges is also still being discussed [12] and needs further investigations.

Acknowledgments: I acknowledge the use of the Planetary Data System (PDS; https://pds.nasa.gov/) and QuickMap (https://quickmap.lroc.asu.edu), a collaboration between NASA, Arizona State University & Applied Coherent Technology Corp.

References:

[1] Lucchitta, B. K. (1976) *LPSC, 7,* 2761–2782. [2] Yue, Z. et al. (2015) *J. Geophys. Res. Planets., 120*, 978–994. [3] Thompson, T. J. et al. (2017) *LPSC, 48,* #2665. [4] Strom, R. G. (1972) *The Moon, 47,* 187–215. [5] Plescia, J. B. and Golombek, M. P. (1986) *Bull. Geol. Soc. Am., 97,* 1289–1299. [6] Watters, T. R. (1988) *J. Geophys. Res., 93,* 10236–10254. [7] Watters, T. R. and Johnson, C. (2009) *Planetary Tectonics*, 121-182. [8] Gold, T. (1972) *The Moon, 47,* 55–67. [9] Fagin, S. W. et al. (1978) *LPSC, 9,* 3473–3479. [10] Yue, Z. et al. (2017) *Earth Planet. Sci. Lett., 477,* 14–20. [11] Valantinas, A. et al. (2017) *Eur. Planet. Sci. Congr., 11,* 961. [12] Valantinas, A. and Schultz, P. H. (2020) *Geology, 48,* 649–653. [13] French, R. A. et al. (2019) *J. Geophys. Res. Planets, 124.* [14] Lu, Y. et al. (2019) *Icarus, 329,* 24–33. [15] Van der Bogert, C. H. et al. (2018) *Icarus, 306,* 225–42. [16] Watters, T. R. et al. (2010) *Science, 329,* 936–940. [17] Watters, T. R. et al. (2012) *Nat. Geosci., 5,* 181–185. [18] Williams, N. R. et al. (2019) *Icarus, 326,* 151–161. [19] Barker, M. K. et al. (2016) *Icarus, 273,* 346–355. [20] Trask, N. J. (1971) *Geol. Surv. Res.,* 138-144. [21] Arvidson, R. et al. (1975) *Moon, 13,* 67–79. [22] Hiesinger, H. et al. (2000) *J. Geophys. Res., 105,* 29239–29275. [23] Valantinas, A. et al. (2018) *Meteorit Planet. Sci., 53,* 826–838. [24] Früh, T. et al. (2020) *LPSC, 51,* #1854. [25] Freed, A. M. et al. (2001) *J. Geophys. Res., 106,* 20603–20620. [26] Watters, T. R. et al. (2015) *Geology, 43,* 851–854. [27] Watters, T. R. et al. (2019) *Nat. Geosci., 12,* 411–417.